Global Change Biology (2009) **15**, 1127–1140, doi: 10.1111/j.1365-2486.2008.01802.x

Response of isoprene emission to ambient CO_2 changes and implications for global budgets

COLETTE L. HEALD*, MICHAEL J. WILKINSON†, RUSSELL K. MONSON†‡, CLEMENT A. ALO§, GUILING WANG§ and ALEX GUENTHER¶

*Department of Atmospheric Science, Colorado State University, Fort Collins, CO, USA, †Department of Ecology and Environmental Biology, University of Colorado, Boulder, CO, USA, ‡Cooperative Institute for Research in Environmental Sciences, University of Colorado, Boulder, CO, USA, §Department of Civil and Environmental Engineering, University of Connecticut, Storrs, CN, USA, ¶Atmospheric Chemistry Division, National Center for Atmospheric Research, Boulder, CO, USA

Abstract

We explore the potential role of atmospheric carbon dioxide (CO_2) on isoprene emissions using a global coupled land–atmosphere model [Community Atmospheric Model–Community Land Model (CAM–CLM)] for recent (year 2000, 365 ppm CO_2) and future (year 2100, 717 ppm CO_2) conditions. We incorporate an empirical model of observed isoprene emissions response to both ambient CO_2 concentrations in the long-term growth environment and short-term changes in intercellular CO_2 concentrations into the MEGAN biogenic emission model embedded within the CLM. Accounting for CO_2 inhibition has little impact on predictions of present-day global isoprene emission (increase from 508 to 523 Tg C yr^{-1}). However, the large increases in future isoprene emissions typically predicted in models, which are due to a projected warmer climate, are entirely offset by including the CO_2 effects. Projected global isoprene emissions in 2100 drop from 696 to 479 Tg C yr^{-1} when this effect is included, maintaining future isoprene sources at levels similar to present day. The isoprene emission response to CO_2 is dominated by the long-term growth environment effect, with modulations of 10% or less due to the variability in intercellular CO_2 concentration. As a result, perturbations to isoprene emissions associated with changes in ambient CO_2 are largely aseasonal, with little diurnal variability. Future isoprene emissions increase by more than a factor of two in 2100 (to 1242 Tg C yr^{-1}) when projected changes in vegetation distribution and leaf area density are included. Changing land cover and the role of nutrient limitation on CO_2 fertilization therefore remain the largest source of uncertainty in isoprene emission prediction. Although future projections suggest a compensatory balance between the effects of temperature and CO_2 on isoprene emission, the enhancement of isoprene emission due to lower ambient CO_2 concentrations did not compensate for the effect of cooler temperatures over the last 400 thousand years of the geologic record (including the Last Glacial Maximum).

Keywords: 2100, CAM, carbon dioxide, climate change, CLM, emission, isoprene, MEGAN, Vostok

Received 9 May 2008 and accepted 28 August 2008

Introduction

Isoprene (C_5H_8, 1-methyl-1,3-butadiene) makes up the largest fraction of nonmethane isatile organic compounds emitted into the atmosphere, with an estimated global source of 440–660 Tg C yr^{-1} (Guenther *et al*., 2006). This highly reactive compound plays a key role in tropospheric chemistry and climate, as a precursor to both ozone (Wang & Shallcross, 2000) and secondary organic aerosol formation (Kroll *et al*., 2006), and as a control over the lifetime of tropospheric methane (Kaplan *et al*., 2006). The dominant isoprene source (>90%) is emission from vegetation, and these emissions are highly sensitive to temperature (Monson *et al*., 1992). Thus, not only does isoprene emission influence climate, but also climate influences isoprene emission, thereby representing an important climate-driven feed-

Correspondence: Colette L. Heald, tel. +1 970 491 8034, fax +1 970 491 8384, e-mail: heald@atmos.colostate.edu

back between photochemical processes in the atmosphere and biogeochemical processes in the terrestrial biosphere. Understanding the isoprene emission response to the meteorological and phenological environment is vital to predicting the evolution of tropospheric composition and climate forcing. Here, we investigate the implications of the isoprene response to changes in atmospheric carbon dioxide (CO_2) concentrations on present day and future global isoprene budgets.

Isoprene emission rates from plants were first measured by Sanadze (1959), and placed into the context of global atmospheric processes by Rasmussen & Went (1965) and have since been characterized for a range of ecosystems via enclosure studies (as summarized by Wiedinmyer *et al*., 2004). Several theories have been offered to explain the role of isoprene biosynthesis in plant processes, including thermal protection (Sharkey & Singsaas, 1995), protection against ozone damage (Loreto *et al*., 2001) and a 'safety valve mechanism' to maintain metabolic homeostasis (Rosenstiel *et al*., 2004). Although individual factors have been shown to dictate the behavior of individual species, for example (Behnke *et al*., 2007), the ultimate reasons(s) for isoprene production in all plants remains unresolved. However, several controlling environmental factors have been identified. Early work recognized the temperature and light sensitivity of isoprene emission and these meteorological drivers were the basis of the first empirical emission models (Tingey *et al*., 1981; Guenther *et al*., 1991, 1993; Lamb *et al*., 1993). Isoprene emissions respond exponentially to short-term (minute-to-minute) increases in temperature (up to a threshold in the range of 40–50 °C) (Monson & Fall, 1989; Singsaas *et al*., 1999) as well as to longer term (weekly-to-seasonal) increases in temperature (Monson *et al*., 1994; Sharkey *et al*., 1999; Petron *et al*., 2001) which contributes to the large seasonal and interannual variability in emission rate at temperate latitudes (Abbot *et al*., 2003), and implies emission increases in the face of global warming (Liao *et al*., 2006). The observed (Pegoraro *et al*., 2004) inhibition of isoprene emission in drought conditions and in young or aged leaves is also included in the recent Model of Emissions of Gases and Aerosols from Nature (MEGAN) (Guenther *et al*., 2006). Additional factors that may modulate isoprene emissions, such as nutrient availability, physical stress and ozone exposure (Harley *et al*., 1994; Alessio *et al*., 2004; Velikova *et al*., 2005), are not included in current emission algorithms, largely due to insufficient data (Guenther *et al*., 2006).

Several studies have shown that elevated atmospheric CO_2 concentration inhibits isoprene production, as summarized by Arneth *et al*. (2007b). This suggests a potential self-regulation of isoprene emission in plants, where in a warmer climate, CO_2-rich atmosphere emissions of isoprene remain relatively unperturbed. Indeed, Arneth *et al*. (2007a) used a process-based isoprene emission model to show that predicted isoprene emission enhancements induced by temperature and vegetation increases in 2100 were offset by inhibition due to ambient CO_2 levels. The direct process-based response of isoprene emission to ambient CO_2 concentrations in this model followed the same behavior predicted by Possell *et al*. (2005) who developed a parameterized response based on a number of plant studies. In a recent study by Wilkinson *et al*. (2008) (hereafter referred to as W08), the first attempt was made to separate and model (1) the long-term response of plants to CO_2 concentrations in the growth environment and (2) the instantaneous response of isoprene emissions to changes in intercellular CO_2 concentration (C_i) when atmospheric CO_2 concentrations are varied in a gas-exchange cuvette. The latter is a function of the balance between leaf CO_2 assimilation rate and leaf stomatal resistance, and can be affected by drought, leaf temperature and light intensity. On the basis of observed responses to both the short-term and the long-term CO_2 levels, W08 developed separate empirical scaling factors for basal emission rates of the form used by Guenther *et al*. (2006). Here, we go beyond previous work by using these scaling factors to test the growth and instantaneous CO_2 effects on simulated global isoprene emissions.

Reduction in isoprene emission potential from exposure to elevated CO_2 may be counter-acted to some degree by the fertilization effect of CO_2 which enhances photosynthesis, water use efficiency and hence vegetation productivity (Drake *et al*., 1997; Körner, 2000). This suggests that in a CO_2-rich atmosphere, net primary productivity (NPP) may increase, but the direct inhibition due to elevated CO_2 concentration will also increase. Furthermore, changes in global land cover may shift the isoprene emission regions northwards with the expansion of the boreal forests (Lathière *et al*., 2005), placing isoprene-emitting forests into a cooler climate.

Predicted changes in isoprene emissions are predicated on an accurate model description of isoprene production, vegetation distribution and future climatic conditions, and are therefore highly uncertain. And yet, the increase in isoprene emission in a warmer climate is among the most important drivers of change in atmospheric chemical composition and oxidative capacity projected by models (Brasseur *et al*., 2006; Liao *et al*., 2006). Past projections of change in isoprene emission, and therefore atmospheric photochemistry in general, have been made using models that emphasize the effects of future climate warming on the highly temperature-sensitive biochemical processes underlying isoprene biosynthesis and/or change in NPP due to

increases in atmospheric CO_2 concentration (Constable *et al*., 1999; Tao & Jain, 2005). Using such models, rising isoprene production in plants is predicted to propel surface ozone levels upwards by 10–30 ppb in the next 100 years, with associated exceedance of air quality standards in some regions (Sanderson *et al*., 2003). The methane lifetime is also projected to increase in a warmer climate as a result of increased competition with isoprene for oxidative radicals (Shindell *et al*., 2007), although there are uncertainties in our understanding of the impact of isoprene on atmospheric oxidation capacity (Lelieveld *et al*., 2008). Enhanced isoprene emission is also projected to increase the burden of biogenic secondary organic aerosols by 20% by the year 2100 (Heald *et al*., 2008). Monson *et al*. (2007) have criticized this approach as ignoring the potential direct effects of increases in atmospheric CO_2 on isoprene. In this study, we use a global coupled land–atmosphere model, along with recently derived models at the leaf level that describe long- and short-term CO_2 effects, to explore the degree to which the inhibition of isoprene emissions under elevated CO_2 concentrations opposes the large increases in isoprene emission predicted for future climate warming scenarios and in the presence of increased global NPP.

Model description

We use here the coupled Community Atmospheric Model (CAM3) and Community Land Model (CLM3.5) of the global NCAR Community Climate System Model (CCSM3) (Collins *et al*., 2006). The CLM simulation is driven by the CCSM-simulated climate. The CAM is run in prognostic mode for present-day (2000) and future (2100) conditions. Simulations are performed with a 30 min time step at a $2^\circ \times 2.5^\circ$ horizontal resolution with 26 vertical levels from the surface to the lower stratosphere ($\sim$ 4 Pa).

The CLM simulates the biogeophysical processes associated with land–atmosphere exchange (Dickinson *et al*., 2006). Vegetation is described by 16 plant functional types (PFTs). Thornton & Zimmermann (2007) provide details on the canopy scheme and how simulated NPP for the CLM model shows generally good agreement with global observations across a range of vegetation types. We use the diagnostic CLM mode, with fixed land surface parameters and with the same spatial and temporal resolution of CAM3. The latest version of CLM (v3.5) surface datasets include leaf area index (LAI) based on MODIS v4 and PFT distributions for present day from a combination of MODIS, AVHRR and crop data as described by Lawrence & Chase (2007). For the set of future simulations which include the effects of land cover change and CO_2 fertilization, we use surface data from the dynamic vegetation CLM simulation of Alo & Wang (2008) (see 'Future projections (2100) with fixed vegetation' for further details). CLM photosynthesis is based on the dePury & Farquhar (1997) sun–shade model, which is a big leaf model that dynamically treats sunlit and shaded photosynthesis and irradiance separately and thus achieves good agreement with more complex multilayer canopy flux models. Photosynthesis rates (A) are dependent on vegetation surface temperature, CO_2 concentrations at the source of carboxylation (after accounting for estimated internal cellular resistance), soil moisture and irradiance. Intercellular CO_2 concentrations within the leaf (C_i) are controlled by leaf boundary layer resistance (r_b) and stomatal resistance (r_s). The Ball–Berry model (Ball *et al*., 1987) is used in CLM as follows:

$$A = \frac{C_a - C_s}{1.37 r_b P_{atm}} = \frac{C_s - C_i}{1.65 r_s P_{atm}}, \quad (1)$$

where C_s is the concentration of CO_2 at leaf surface, C_a is the atmospheric concentration of CO_2 and P_{atm} is the atmospheric pressure. Leaf boundary resistance (r_b) is calculated as a function of wind speed after fixing the leaf-to-air turbulent transfer coefficient at 0.01 m $s^{-1/2}$ and the characteristic leaf dimension at 0.04 m (following the procedures described in Oleson *et al*. (2004). Stomatal resistance is solved iteratively based on rates of photosynthesis, and C_i is then resolved following Eqn (1) (Oleson *et al*., 2004).

Future climate conditions are based upon the IPCC SRES A1B scenario (IPCC, 2001), with atmospheric CO_2 concentrations fixed at 717 ppm for the year 2100. Present-day (which we take as the year 2000) CO_2 concentrations are fixed at 365 ppm. Sea surface temperatures are specified from previous NCAR CCSM climate change experiments using the SRES A1B emissions (Meehl *et al*., 2006). The transient climate sensitivity of the CCSM3 fully coupled model is 2.47 °C (Kiehl *et al*., 2006). A full analysis of the CCSM3 future climate simulation is not the objective of this work, see Meehl *et al*. (2006) for further details.

All analyzed simulations are initialized following a 1-year spin-up simulation. Future snapshot simulations are performed for 1 year and are repeated for 10 years to assess the magnitude of interannual climate variability in the vicinity of the snapshot. We perform three sets of simulations here: (1) present-day vegetation and climate (2000), (2) future climate with fixed vegetation and (3) future climate with projected 2100 vegetation. We use the fixed vegetation simulations as our standard present-day and future simulations.

Algorithm description

MEGAN v2 isoprene emission scheme

Isoprene emissions in CLM follow the MEGAN v2.0 with detailed canopy light and temperature algorithms (Guenther *et al*., 2006). Basal emission factors (ε_j) at standard conditions of light, temperature and leaf area are specified for each PFT (j), for each grid box to account for species-wide divergence in emission capacities. Total canopy-level fluxes (F, in units of $\mu g\,C\,m^{-2}\,h^{-1}$) are calculated by summing the emissions across all vegetation types with fractional area coverage (χ_j) in the grid box and modulating the basal emission rate with an emission activity factor (γ):

$$F = \gamma\rho\sum_j \varepsilon_j\chi_j, \tag{2}$$

where ρ is the canopy loss and production factor, set here to unity, as recommended for isoprene by Guenther *et al*. (2006).

The activity factor accounts for emissions response to phenological and meteorological conditions and includes scaling factors for light (γ_P), temperature (γ_T), leaf age (γ_{age}), soil moisture (γ_{SM}) and LAI:

$$\gamma = C_{CE}LAI\gamma_P\gamma_T\gamma_{age}\gamma_{SM}, \tag{3}$$

The activity factors in Eqn (3) are calculated based on the instantaneous temperature, radiation, soil moisture and LAI at each time step in the CLM, as well as the average temperature and radiation conditions over the last 24 h and 10 days. The radiation response is applied separately for the sunlit and shaded leaves in the forest canopy environment. The canopy environment constant (C_{CE}), a factor used to set emission activity to unity at standard conditions, is set to 0.40 for the CLM model at the standard conditions specified by Guenther *et al*. (2006).

Activity factor for the CO_2 response

Recent studies have shown a significant inhibition of isoprene emission rate in the presence of elevated atmospheric CO_2 concentration for several species plants and for both short-term exposure (affecting C_i) and long-term exposure (due to increase in C_a) as summarized by Arneth *et al*. (2007b). Recently, W08 described a series of experiments using four plant species *Populos tremuloides* (aspen), *Populos deltoides* (cottonwood), *Liquidambar styraciflua* (sweetgum) and *Eucalyptus globulus* (eucalyptus), in which, once again, a consistent inhibition of isoprene emission rate was shown in the presence of elevated C_i over the short term and C_a over the longer term. In that study, a model was developed to describe both the short- and long-term response to CO_2 separately based on the observed response of the aspen plants, for which a greater number of growth environment experiments were performed. We use this model to describe the generalized CO_2 response for all isoprene-emitting vegetation in the global analysis reported here. We note that this is a simplification and requires the assumption that all isoprene-emitting species function in the same way with regard to CO_2 sensitivity. The parameterization may be expanded as further plant species are tested for their CO_2 sensitivity; it is particularly important that tropical plants are investigated as they dominate most global inventories of the total isoprene flux. In support of our simplification, however, we note that both Possell *et al*. (2005) and W08 find that a number of different herbaceous and woody species respond consistently to changes in the atmospheric CO_2 concentration, and thus the parameterized response observed by W08 may indeed provide an adequate description of midlatitude or even global vegetation.

W08 find that isoprene emission rates decrease nonlinearly with instantaneous changes in intercellular CO_2 concentration. They suggest that this response can likely be linked to changes in metabolite pools and enzyme activity within the leaf. The activity factor (γ_{C_i}) is modeled as a sigmoidal response curve:

$$\gamma_{C_i} = I_{s\max} - \left[\frac{I_{s\max}(C_i)^h}{(C^*)^h + (C_i)^h}\right], \tag{4}$$

where $I_{s,max}$ is the estimated asymptote at which further decreases in intercellular CO_2 have a negligible effect on isoprene emission, C^* is a scaling coefficient and h is an exponential scalar. The sensitivity of isoprene emission rate to C_i decreases with long-term exposure to elevated atmospheric CO_2; thus, isoprene emission response curves are fit individually to the responses reported in W08 for plants grown at 400, 600, 800 and 1200 ppmv atmospheric CO_2 (W08, Fig. 5). The parameters for Eqn (4) were obtained from these response curves and are provided in Table 1.

Enhanced CO_2 concentrations in the long-term growth environment of the plant were also found to induce a negative response in isoprene synthesis, likely the result of changes in gene expression in the plant (W08). This response exhibited the same sigmoidal functionality as the short-term response:

$$\gamma_{C_a} = I_{s\max} - \left[\frac{I_{s\max}(0.7C_a)^h}{(C^*)^h + (0.7C_a)^h}\right]. \tag{5}$$

The parameters for Eqn (5) are given in Table 2. Note that W08 defined these parameters as a function of C_i,

Table 1 Empirically determined parameter values for Eqn (4) (short-term isoprene emission response to intercellular CO_2) from aspen trees (W08)

Long-term growth CO_2 treatment (ppmv)	$I_{s\ max}$	h	C^*
400	1.072	1.7000	1218
600	1.036	2.0125	1150
800	1.046	1.5380	2025
1200	1.014	2.8610	1525

Table 2 Empirically determined parameter values for Eqn (5) (long-term isoprene emission response to growth environment atmospheric CO_2) from aspen trees (W08)

$I_{s\ max}$	h	C^*
1.344	1.4614	585

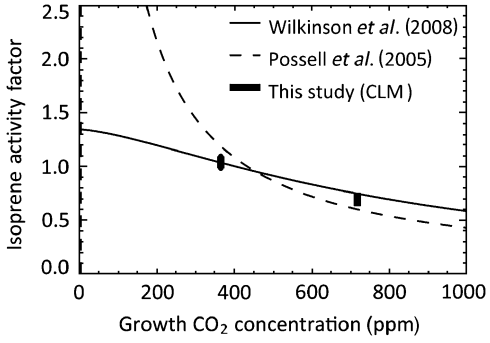

Fig. 1 Changes in normalized isoprene emission rates with growth atmospheric CO_2 concentration. The long-term growth environment fit from Wilkinson *et al*. (2008) is compared with the parameterization of Possell *et al*. (2005). Also shown are the range in monthly mean activity factors simulated here with Community Atmospheric Model (CLM) in all vegetated grid boxes, in 2000 ($C_a = 365$ ppm) and 2100 ($C_a = 717$ ppm) when both the long-term and short-term effects of CO_2 on isoprene emission are included. Standard conditions are defined as 400 ppm ambient CO_2 concentrations for W08 and 366 ppm for Possell *et al*. (2005).

which they assumed was equivalent to 0.7 of the observed atmospheric CO_2 concentration (C_a) and we include this conversion in Eqn (5). W08 show how this parameterization agrees well with the response estimated by Possell *et al*. (2005) over the range of atmospheric CO_2 concentrations considered (but diverges at $C_a < 400$ ppm), as shown here in Fig. 1. The parameterization of Possell *et al*. (2005) gives isoprene emission activity factors of 1.19 and 0.60 for atmospheric CO_2 concentrations of 365 ppm and 717 ppm, respectively, implying a 49% decrease in isoprene emission efficiency from 2000 to 2100. Conversely, the long-term growth environment parameterization of W08 implies a 28% drop in efficiency (activity factors of 1.04 and 0.75 for 365 ppm and 717 ppm, respectively), and if C_i is assumed to be 0.7 of C_a globally, then the additional short-term effect yields a total 37% decrease in isoprene emission efficiency.

The activity factors for the CO_2 response are implemented in the CLM MEGAN2 emission scheme described in 'MEGAN v2 isoprene emission scheme' as additional activity factors in Eqn (3). The parameters for Eqn (4) are obtained by linearly interpolating the values in Table 1 corresponding to intervals of long-term growth CO_2 concentration to the specified atmospheric CO_2 concentration. Within CLM, the short-term activity factor (γ_{C_i}) is then calculated following Eqn (4) based on simulated instantaneous C_i at each location and timestep. The activity factor for long-term growth environment (γ_{C_a}) is calculated from Eqn (5) given a fixed atmospheric CO_2 concentration and is globally constant in these simulations. In the sections that follow, the short-term and long-term activities factors are treated as one single activity factor ($\gamma_C = \gamma_{C_i}\gamma_{C_a}$) for all figures.

Global isoprene budgets

Present-day (2000)

Figure 2 shows the seasonal distribution of simulated C_i and the CO_2 activity factors, which generally range between 1.01 and 1.05 for present-day conditions, over different latitude bands. The activity factor associated with long-term exposure to CO_2 concentrations of 365 ppm derived from Eqn (5) is 1.04. This value is greater than unity because CO_2 concentrations are less than the standard conditions of 400 ppm. The activity factor for short-term CO_2 exposure is within 5% of unity. The range of simulated activity factors (for both long- and short-term effects together) in 2000 is plotted on Fig. 1, and agrees well with both W08 and Possell *et al*. (2005) fits. The net result of both activity factors is a slight increase (3%) in global isoprene emissions from 508 Tg C yr^{-1} with standard MEGAN2 to 523 Tg C yr^{-1} when CO_2 activity factors are included (Table 3). This increase is significant when compared with the simulated variability in global total isoprene emissions due to interannual variability in climate (standard deviation of ± 8 Tg C yr^{-1} in global total emissions over the 10-year simulation). Relative emission increases are fairly uniform globally, with the largest absolute increases in Australia, sub Saharan Africa and South America (Fig. 3). Figure 4 shows that the CO_2 activity factor is largely aseasonal, compared with the other meteorological and phenological activity factors of Eqn (3).

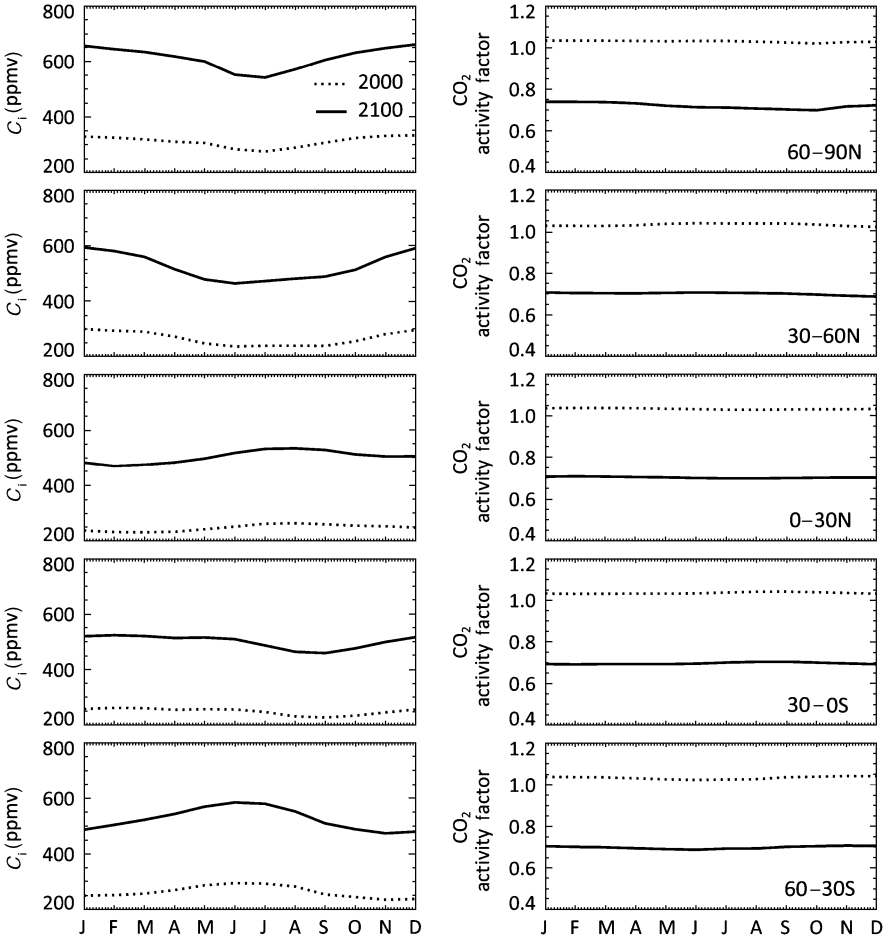

Fig. 2 Seasonal cycle of mean intercellular CO_2 concentrations (C_i, left) and carbon dioxide activity factor (γ_C, right) over five latitude bands. Values are contrasted for 2000 (dotted lines) and 2100 with fixed vegetation (solid lines).

Future projections (2100) with fixed vegetation

Atmospheric CO_2 concentrations in 2100 (717 ppm) result in a 0.75 isoprene emission activity factor (or 25% reduction) associated with long-term growth environment following Eqn (5) (Fig. 2). The short-term response yields activity factors of 0.86–1.03 depending on local C_i (see further discussion below), which when combined with the long-term effect, results in a significant net reduction in simulated isoprene emissions compared with the standard MEGAN2 [as described by Eqn (3)]. Global total emissions drop 31% from 696 to 479 Tg C yr^{-1} (Table 3, Fig. 3). Relative emission reductions are generally globally uniform. Figure 3, therefore, shows that the largest absolute changes in isoprene emission when analyzed with the CO_2 activity factor included in the model are found in the largest isoprene emission regions, in Australia, sub-Saharan Africa and the Amazon region of South America.

Table 3 Isoprene Emission (Tg C yr^{-1}) simulated using CLM

Year	Standard MEGAN2	MEGAN2 with CO_2 activity factor
2000	508	523
2100 (A1B) with fixed vegetation	696	479
2100 (A1B) with dynamic vegetation	1852	1242

CLM, Community Land Model; MEGAN, Model of Emissions of Gases and Aerosols from Nature.

Figure 5 shows the seasonal simulated CO_2 activity factors, C_i (normalized by C_a) and the factors which control these concentrations for the year 2100. Controlling factors included the rate of photosynthesis and stomatal resistance. For example, increased photosynthesis rates (e.g. throughout Russia in summer) have the effect of consuming atmospheric CO_2 and therefore

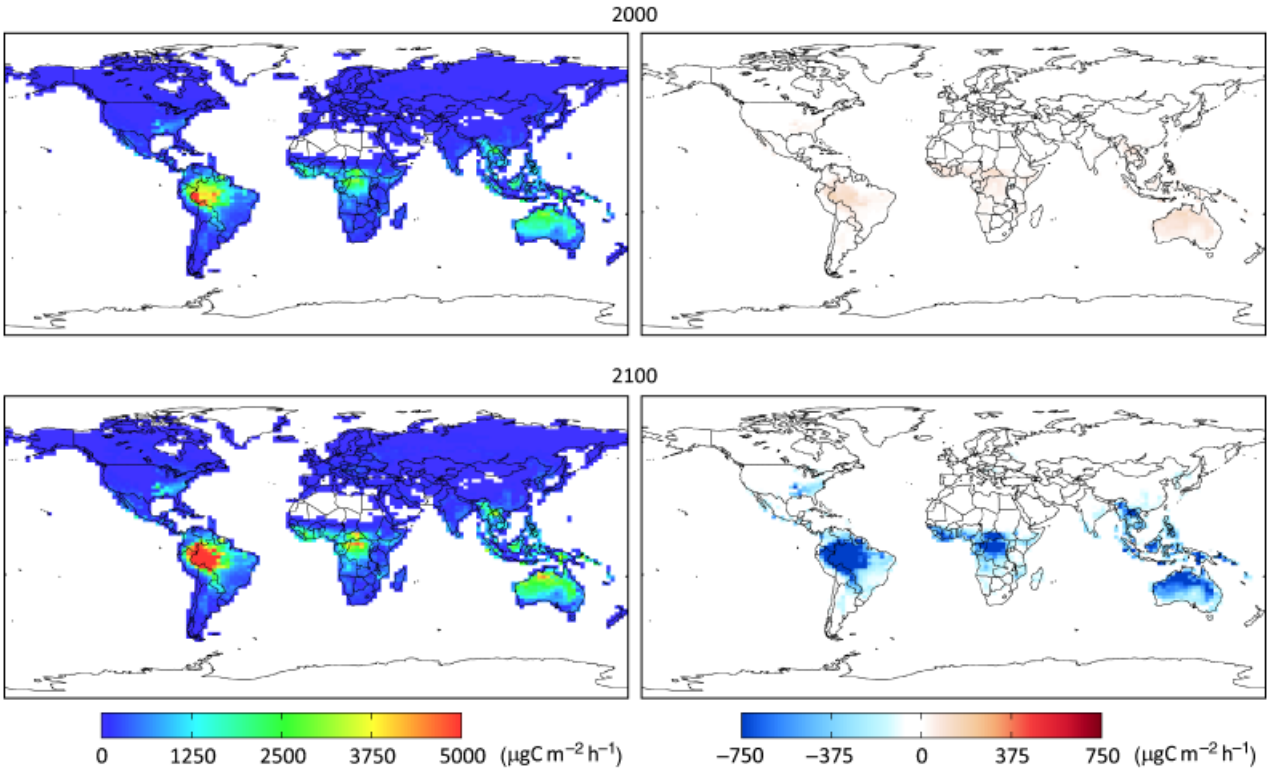

Fig. 3 Annual present-day (2000, top row) and future (2100, bottom row) simulated mean isoprene emissions without CO_2 activity factor (left) and difference in emission when CO_2 activity factor is included (right). Color scales are saturated at respective values.

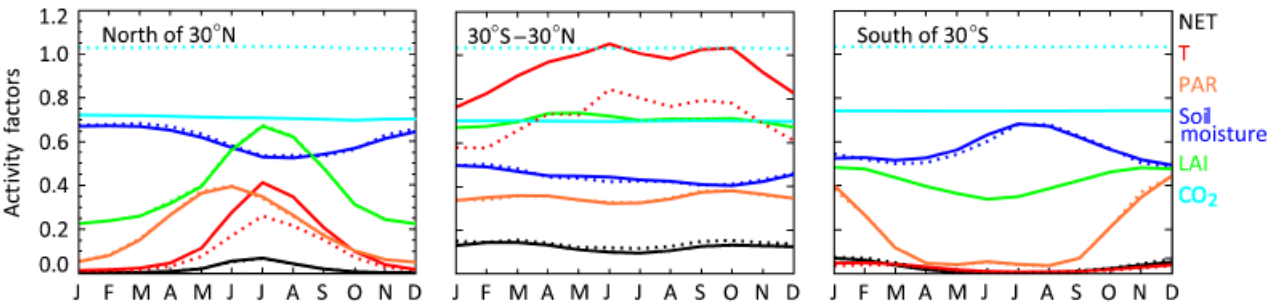

Fig. 4 Present day (2000, dotted lines) and future with fixed vegetation (2100, solid lines) seasonal cycle of mean isoprene emission activity factors North of 30°N (left), in the tropics (center) and South of 30°S (right).

they also cause decreases in C_i within the leaf [as predicted by Eqn (1)]. Similarly, increased stomatal resistance impedes the diffusion of CO_2 from the atmosphere into the leaf, also forcing a reduction in C_i. The seasonal variability in C_i due to the interacting effects of photosynthesis and stomatal resistance are apparent over the boreal forests of the northern high latitudes, where isoprene sources are less abundant compared with temperate and tropical latitudes. We note that although the average ratio of C_i to C_a is close to 0.7 as assumed by W08, there is significant regional variability (Fig. 5). However, in general, the activity factor associated with the CO_2 effect varies little, particularly when compared with the seasonal response to light and temperature (Fig. 4). The nearly constant response of isoprene emission rate to CO_2 is a consequence of the dominance of the long-term growth CO_2 response over the short-term C_i-driven response. As seen in Fig. 1, the global variability in simulated isoprene emission response to C_i is nominal on a monthly mean basis.

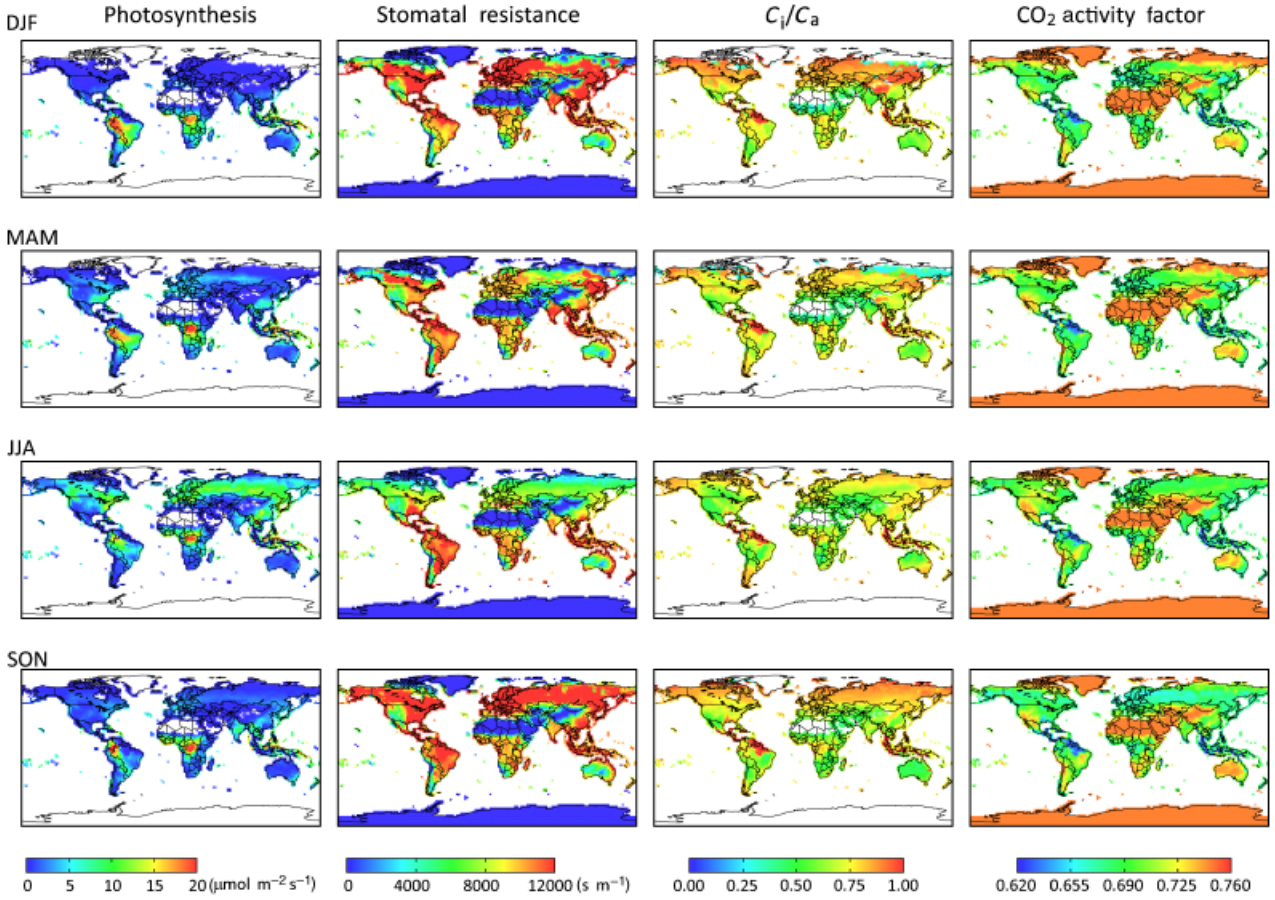

Fig. 5 Seasonal mean distribution of future (2100) simulated photosynthesis, stomatal resistance, intercellular CO_2 concentrations (C_i normalized by atmospheric CO_2 concentrations C_a) and resulting CO_2 activity factor with fixed vegetation. Color scales are saturated at respective values.

Despite the large range of simulated C_i around the world shown in Fig. 5, the resulting sensitivity of isoprene emissions generally varies by less than 10% in 2100. In addition, the mean response to C_i is generally a 10% decrease in isoprene emission or less. In fact, this simulation suggests that the discrepancy between the two model fits (Possell *et al*., 2005 vs. W08) may be resolved by accounting for the short-term C_i-driven response. The fits of Possell *et al*. (2005) and W08 differ by $\sim$ 10% in 2100, including the short-term response reduces the W08 prediction by close to this amount, bringing the results into closer agreement.

Although the seasonal role of C_i variability is small, the diurnal response may be important at local scales. To test this, we examine the diurnal profile of C_i and the associated CO_2 activity factor in two important isoprene source regions: North and South America. Figure 6 shows both the mean and range of activity factors associated with C_i (normalized by C_a) in summer (June–August) of 2100. Again, we illustrate here that a large range in C_i translates to modest differences in activity factor. Above all, this figure shows that C_i does not vary sufficiently on a diurnal basis to significantly modify isoprene emission, at least at the local landscape scale. We compare the diurnal variability in activity factor associated with changes in CO_2 concentration with that associated with light to make this distinction.

Interplay between drought and C_i likely exists in certain environments as the maximum rate of carboxylation is adversely affected by drought. We hypothesize that decreases in soil moisture could thus scale back isoprene emissions both directly and indirectly (as shown previously by Pegoraro *et al*., 2004). However, as we have shown, differences in C_i do not appreciably alter isoprene emission rates in 2100 using the model of W08. For example, although there are strong seasonal trends in soil moisture in Amazonia which are associated with reduced photosynthesis in the dry season, the resulting differences in C_i (of $\sim$ 100 ppm) modify isoprene emissions by only a few percent.

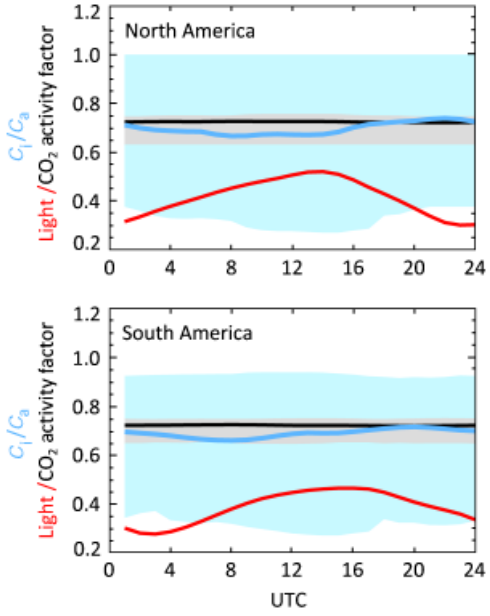

Fig. 6 Diurnal trend in summer (June–August) 2100 mean (line) and range (shaded region) of intercellular CO_2 concentrations (normalized by atmospheric CO_2, blue) and CO_2 activity factor (black) for North America and South America. Also shown is the mean diurnal profile of isoprene emission activity factor associated with light (red).

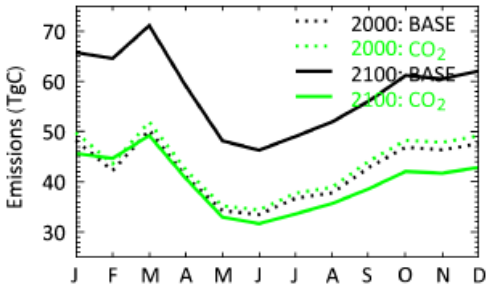

Fig. 7 Seasonal cycle of total global isoprene emissions for present-day (2000, dotted) and future with fixed vegetation (2100, solid) simulation with (green) and without (black) CO_2 activity factor.

Standard MEGAN2 algorithms would predict a 37% increase in isoprene emission from 2000 to 2100, largely a result of rising temperatures (Fig. 7). Figure 4 shows that in this simulation with fixed vegetation, the only activity factor of Eqn (3) predicted to change significantly under future conditions is that related to temperature. In 'Activity factor for the CO_2 response', we noted that if C_i is assumed to be 70% of C_a isoprene emission efficiency due to both the long-term and short-term CO_2 effects decreases by 37% from 2000 to 2100. Thus, the isoprene response to projected increases in temperature and CO_2 would offset each other exactly. However, average C_i in the model is higher than 70% of C_a and therefore the model predicts an 8% decrease in emissions by 2100 (compared with 2000) when the activity factor accounting for CO_2 concentration is included. Projected regional trends match the global average picture, with large increases in isoprene emission rates from 2000 to 2100 due to climate warming, negated by including the inhibition of isoprene emission by CO_2.

Future projections (2100) with predicted vegetation

Dynamic vegetation models generally predict the future degradation of vegetation in Amazonia and the regrowth of the high-latitude boreal forests in concert with a lengthened growing season and associated increases in LAI over vegetated regions (Joos *et al*., 2001; Gerber *et al*., 2004; Lathière *et al*., 2005). Reductions in rainfall may lead to water stress and regional dieback (Niyogi & Xue, 2006). Guenther *et al*. (2006) find that isoprene emissions may decrease by up to 30% when future vegetation distributions are used to drive MEGAN, although this projection is based on a specific land-use change scenario that assumes a very large increase in global cropland area. They also show projections of LAI which more than double in some regions by 2100; this is primarily due to projected increases in NPP. The linear dependence of isoprene emission rate on LAI (which is modulated by a nonlinear decrease due to the light-dependent activity factor γ_P particularly at high LAI), described in Eqn (3), highlights the critical importance of understanding the effects of terrestrial CO_2 fertilization for future prediction of isoprene emission.

To investigate the relative sensitivity of isoprene emission to vegetation distribution and density, we use land surface parameters, including global PFT distribution and LAI, projected with a dynamic global vegetation model (DGVM). Our goal here is not to capture the range in potential vegetation response which can vary significantly with climatic predictions (Alo & Wang, 2008) and among models (Scholze *et al*., 2006), but rather to use a single realization of future vegetation to compare the relative effects of changes in vegetation distribution and productivity vs. the direct effect of CO_2 inhibition on the projected global isoprene emission rate. Alo & Wang (2008) used the CLM DGVM to investigate the response of the terrestrial ecosystem to changes in climate projected by eight general circulation models. We use their results for 2100 under the A1B scenario driven by the climate predictions of the CCSM, consistent with the model and future conditions employed here. Although the global vegetation expansion projected by the CLM DGVM driven by the CCSM climate is consistent with the increases seen in seven of the eight models, regional responses in vegetation may differ. In particular, this model does not project the

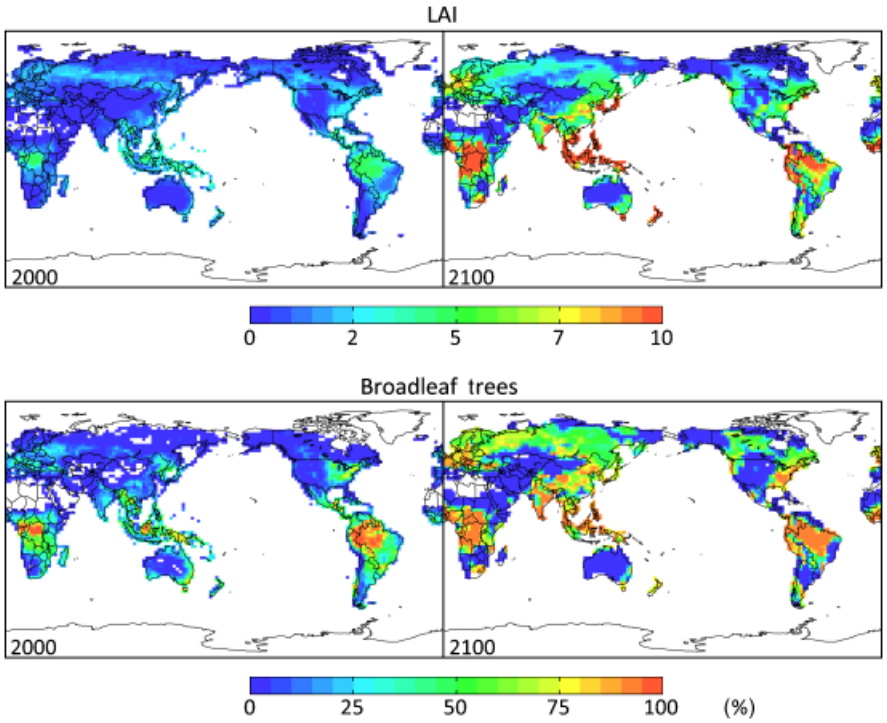

Fig. 8 Comparison of total leaf area index (LAI) (top) and broadleaf tree coverage (bottom) for the year 2000 (left) (Thornton & Zimmermann, 2007) and as predicted by the Community Atmospheric Model (CLM) dynamic vegetation model for 2100 (A1B, right) (Alo & Wang, 2008). Color scales are saturated at respective values.

extensive deforestation of the Amazon projected in some previous studies (Lathière *et al*., 2005) and seen in one model considered by Alo & Wang (2008). The CCSM model predicts wetter conditions in 2100 than any of the other models considered, and thus water limitations do not instigate large-scale vegetation dieback. We note here that these simulations account only for natural changes in vegetation and do not include the effects of urbanization and cropland expansion. Global mean LAI over vegetated surfaces more than triples from 1.2 $m^2 m^{-2}$ in the MODIS-based present-day conditions of Lawrence & Chase (2007) to 3.8 $m^2 m^{-2}$ in the 2100 simulation of Alo & Wang (2008). Figure 8 shows that foliar expansion due to CO_2 fertilization and enhanced NPP is projected throughout the world and is not limited to specific regions. Vegetation cover is projected to increase in general, with a northward expansion as projected in previous studies (Joos *et al*., 2001; Gerber *et al*., 2004; Lathière *et al*., 2005), particularly for broadleaf trees (shown in Fig. 8), the highest emitters of isoprene among PFTs. For further discussion of the potential changes in the terrestrial ecosystem, we refer the reader to Alo & Wang (2008).

When the effects of dynamic vegetation and enhanced NPP from CO_2 fertilization are included, global isoprene production is projected to more than double by 2100 (1240 Tg C yr^{-1}), compared with present-day levels (note that emissions are even higher when CO_2 inhibition is not accounted for, Table 3). This effect is significantly larger than the inhibition of isoprene emission predicted from the results presented in W08. However, recent work has shown that the biosphere's capacity to absorb CO_2 has been overestimated by up to 74% in models which do not account for nutrient limitation (Thornton *et al*., 2007), and thus future LAI increases may be significantly more modest. Indeed, if LAI increases by only a quarter of the predictions of Alo & Wang (2008), isoprene increases associated with this effect would be comparable with decreases due to the direct effect of CO_2 inhibition. Arneth *et al*. (2007a) found that CO_2 inhibition compensated fully for both temperature and vegetation changes projected for 2100 in the LPJ-GUESS model. This substantially different level of compensation likely arises from the use of very different climate drivers, where the study of Arneth *et al*. (2007a) was driven by the one model (HadCM) highlighted by Alo & Wang (2008) to project large decreases in natural vegetation, in stark contrast to the CCSM climate used here.

Implications for historical isoprene emissions

Figure 9 shows how isoprene emission activity factors associated with temperature and CO_2 levels evolved

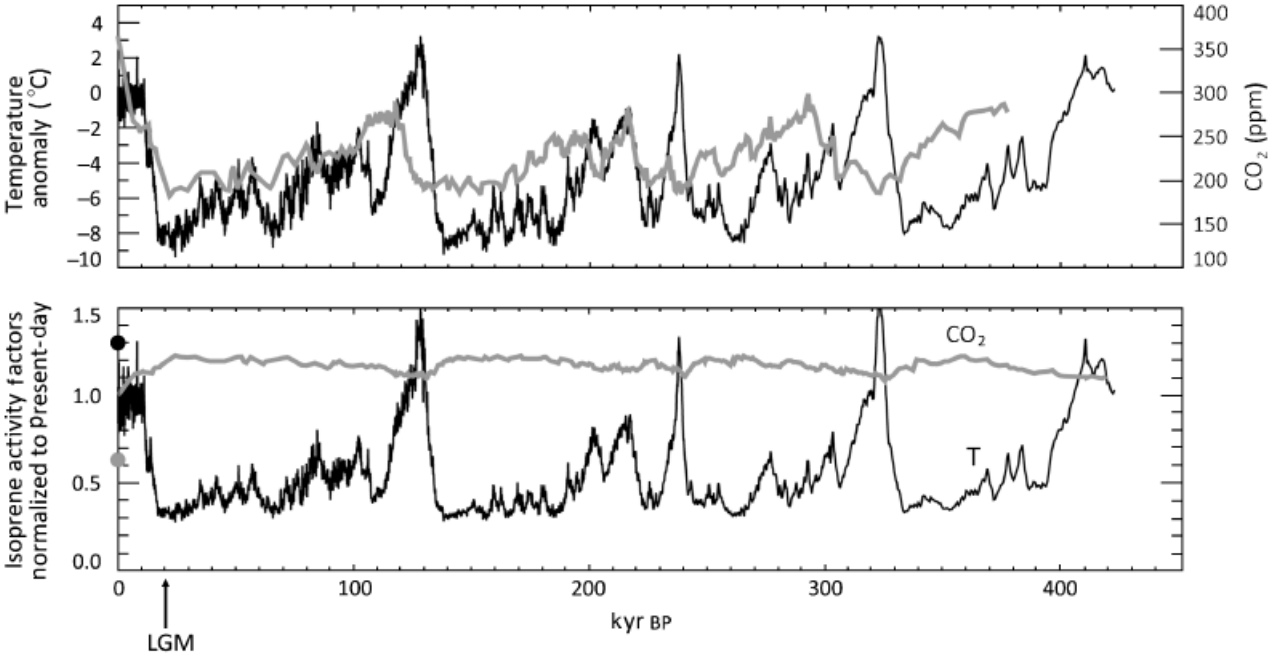

Fig. 9 The geological record of temperature anomaly (black) and atmospheric CO_2 concentrations (grey, thick) from the Vostok ice core (top) and the associated isoprene emission activity factors (below). Activity factors are normalized to present-day values. The CO_2 activity factor includes both long- and short-term effects. The short-term CO_2 activity factor over the geological past depends on parameters for plants grown at 400 ppm in Table 1, as values for lower CO_2 growth environments are not available. Predicted activity factors for 2100 are shown as dots. The Last Glacial Maximum (LGM) is noted. Vostok data source: Petit *et al*. (1999).

throughout the recent geological past. Atmospheric CO_2 concentrations over the Vostok ice core record are lower than present day, and thus isoprene emission is expected to be enhanced by CO_2, not inhibited as seen for future conditions. However, over this time period, atmospheric CO_2 concentrations rarely deviate from concentrations of 150–250 ppm and thus the CO_2 enhancement of isoprene production remains modest and fairly constant. Therefore, although the balance between temperature and CO_2 activity factors is critical to future predictions of isoprene (our results for 2100 are shown as circles on Fig. 9), large temperature fluctuations in the geological past remain the primary control on isoprene emissions over the last 400 thousand years.

Adams *et al*. (2001) and Kaplan *et al*. (2006) suggest that the drop in methane concentrations observed in ice core samples during the Last Glacial Maximum (LGM, $\sim$ 20 000 years BP) could be explained by an enhanced oxidative sink (hydroxyl) resulting from lower isoprene emissions in a cooler climate with reduced vegetation. However, the enhancement of isoprene emission associated with depressed CO_2 concentrations in the past would act against this, perhaps nullifying any effect on OH. Indeed, Arneth *et al*. (2007a) predict a strong CO_2 enhancement at the LGM following the parameterization of Possell *et al*. (2005). However, as seen in Fig. 1, the W08 parameterization shows a much more modest enhancement of isoprene at low CO_2 concentrations which, when compared with the effect of temperature at the LGM (Fig. 9), would imply a net drop in isoprene emission, consistent with the historical record of methane. The divergence of these parameterizations plainly highlights the need for further study of the direct effect of CO_2 on isoprene emission at low concentrations.

Conclusions

We use a global coupled land–atmosphere model here to show that the inhibition of isoprene emission with increasing CO_2 concentrations that has been observed in leaf-level studies is a key control on future projections of global isoprene emission rate. In particular, we find that the CO_2 inhibition predicted in 2100 under the A1B IPCC SRES scenario may completely offset the large temperature-driven increase in isoprene emission predicted by standard models. This suggests that future isoprene production may to a large degree be buffered by competing influences. In contrast to current model prediction, Lelieveld *et al*. (2008) have proposed that tropical forests are able to maintain a strong atmospheric oxidation capacity even while emitting copious

quantities of reactive isoprene. This remarkable capability for sustaining the atmosphere's cleansing ability may be enhanced at millennial scales by the opposing response of isoprene to temperature and CO_2. We note, however, that this simple picture does not account for changing vegetation. Although uncertainty remains as to how effectively CO_2 fertilization might enhance global NPP and how this may be limited by nutrient availability, it is certainly likely that fertilization under higher atmospheric CO_2 concentrations will contribute to foliar expansion. Rising atmospheric CO_2 concentrations are also likely to result in significant changes in species composition (Mohan *et al*., 2007) that will lead to substantially increased isoprene emissions in at least some landscapes. To what degree either of these potential forcings would enhance future isoprene emissions remains unclear.

We find here that the response of isoprene to CO_2 concentrations is dominated by the long-term growth effect. The results of W08 suggest that the shorter-term influences driven by dynamics in C_i modulate isoprene emission by less than 10% under CO_2 concentrations in present day and in a 2100 scenario. Furthermore, the aseasonality of the activity factor associated with C_i throughout most of the world and the consistent diurnal profile imply that this 10% modulation does not introduce important temporal variability in isoprene production. Although the long-term growth parameterization of W08 is easily incorporated in any chemical transport model (CTM), few CTMs are interfaced with an active land model for prognostic estimation of C_i in plants. Our results suggest that neglect of the short-term response of isoprene emission to C_i would imply at most a 10% overestimate in the prediction of isoprene emissions. This falls within existing uncertainties on isoprene emission estimates. Alternatively, given the modest variability in CO_2 activity factor associated with variable C_i, fixing the C_i to a globally constant fraction of C_a (such as 0.7 as previously suggested) in CTMs would adequately describe the short-term response.

The dampening of future predicted isoprene emission increases via CO_2 inhibition points towards a more constant chemical composition of the troposphere than previous projections suggest. The feedback of a warmer climate on isoprene emission from vegetation and the associated anticipated enhancements in ozone, organic aerosol and methane may be significantly muted in a high CO_2 environment.

The W08 parameterization implies that the enhancement of isoprene emission due to low ambient CO_2 concentrations during the LGM ($\sim$ 20 000 years ago) is dwarfed by the effect of the cooler climate. This supports previous conclusions that reductions in glacial isoprene emission may explain some of the glacial–interglacial changes in methane concentrations observed in ice cores.

Acknowledgements

The use of the computing time for the model experiments was supplied through the National Center for Atmospheric Research, Community Climate System Model (CCSM) Chemistry-Climate Group, which is sponsored by the National Science Foundation. R.M. and M.W. acknowledge the support of NSF grant 0543895 and EPA grant RD-831455301. We thank Arlene Fiore for early comments on the manuscript.

References

Abbot DS, Palmer PI, Martin RV, Chance KV, Jacob DJ, Guenther A (2003) Seasonal and interannual variability of North American isoprene emissions as determined by formaldehyde column measurements from space. *Geophysical Research Letters*, **30**, 1886, doi: 10.1029/2003GL017336.

Adams JM, Constable JVH, Guenther AB, Zimmerman P (2001) An estimate of natural volatile organic compound emissions from vegetation since the last glacial maximum. *Chemosphere – Global Change Science*, **3**, 73–91.

Alessio GA, De Lillis M, Fanelli M, Pinelli P, Loreto F (2004) Direct and indirect impacts of fire on isoprenoid emissions from Mediterranean vegetation. *Functional Ecology*, **18**, 357–364.

Alo CA, Wang GL (2008) Potential future changes of the terrestrial ecosystem based on climate projections by eight general circulation models. *Journal of Geophysical Research – Biogeosciences*, **113**, G01004, doi: 10.1029/2007JG000528.

Arneth A, Miller PA, Scholze M, Hickler T, Schurgers G, Smith B, Prentice IC (2007a) CO2 inhibition of global terrestrial isoprene emissions: potential implications for atmospheric chemistry. *Geophysical Research Letters*, **34**, L18813, doi: 10.1029/2007GL030615.

Arneth A, Niinemets U, Pressley S *et al*. (2007b) Process-based estimates of terrestrial ecosystem isoprene emissions: incorporating the effects of a direct CO_2–isoprene interaction. *Atmospheric Chemistry and Physics*, **7**, 31–53.

Ball JT, Woodrow IE, Berry JA), (eds) (1987) *A Model Predicting Stomatal Conductance and Its Contribution to the Control of Photosynthesis Under Different Environmental Conditions*. Martinus Nijhoff, Dordrecht, the Netherlands.

Behnke K, Ehlting B, Teuber M *et al*. (2007) Transgenic, non-isoprene emitting poplars don't like it hot. *Plant Journal*, **51**, 485–499.

Brasseur GP, Schultz M, Granier C *et al*. (2006) Impact of climate change on the future chemical composition of the global troposphere. *Journal of Climate*, **19**, 3932–3951.

Collins WD, Bitz CM, Blackmon ML *et al*. (2006) The Community Climate System Model version 3 (CCSM3). *Journal of Climate*, **19**, 2122–2143.

Constable JVH, Guenther AB, Schimel DS, Monson RK (1999) Modelling changes in VOC emission in response to climate change in the continental United States. *Global Change Biology*, **5**, 791–806.

dePury DGG, Farquhar GD (1997) Simple scaling of photosynthesis from leaves to canopies without the errors of big-leaf models. *Plant Cell and Environment*, **20**, 537–557.

Dickinson RE, Oleson KW, Bonan G *et al*. (2006) The community land model and its climate statistics as a component of the community climate system model. *Journal of Climate*, **19**, 2302–2324.

Drake BG, GonzalezMeler MA, Long SP (1997) More efficient plants: a consequence of rising atmospheric CO_2? *Annual Review of Plant Physiology and Plant Molecular Biology*, **48**, 609–639.

Gerber S, Joos F, Prentice IC (2004) Sensitivity of a dynamic global vegetation model to climate and atmospheric CO_2. *Global Change Biology*, **10**, 1223–1239.

Guenther A, Karl T, Harley P, Wiedinmyer C, Palmer PI, Geron C (2006) Estimates of global terrestrial isoprene emissions using MEGAN (Model of Emissions of Gases and Aerosols from Nature). *Atmospheric Chemistry and Physics*, **6**, 3181–3210.

Guenther AB, Monson RK, Fall R (1991) Isoprene and monoterpenes emission rate variability – observations with eucalyptus and emission rate algorithm development. *Journal of Geophysical Research – Atmospheres*, **96**, 10799–10808.

Guenther AB, Zimmerman PR, Harley PC, Monson RK, Fall R (1993) Isoprene and monoterpene emission rate variability – model evaluations and sensitivity analyses. *Journal of Geophysical Research – Atmospheres*, **98**, 12609–12617.

Harley PC, Litvak ME, Sharkey TD, Monson RK (1994) Isoprene emission from velvet bean leaves – interactions among nitrogen availability, growth photon flux density, and leaf development. *Plant Physiology*, **105**, 279–285.

Heald CL, Henze DK, Horowitz LW *et al*. (2008) Predicted change in global secondary organic aerosol concentrations in response to future climate, emissions, and land use change. *Journal of Geophysical Research – Atmospheres*, **113**, D05211, doi: 10.1029/2007JD009092.

IPCC (2001) *Climate Change 2001: The Scientific Basis*. Cambridge University Press, Cambridge, UK.

Joos F, Prentice IC, Sitch S *et al*. (2001) Global warming feedbacks on terrestrial carbon uptake under the Intergovernmental Panel on Climate Change (IPCC) emission scenarios. *Global Biogeochemical Cycles*, **15**, 891–907.

Kaplan JO, Folberth G, Hauglustaine DA (2006) Role of methane and biogenic volatile organic compound sources in late glacial and Holocene fluctuations of atmospheric methane concentrations. *Global Biogeochemical Cycles*, **20**, GB2016, doi: 10.1029/2005GB002590.

Kiehl JT, Shields CA, Hack JJ, Collins WD (2006) The climate sensitivity of the Community Climate System Model version 3 (CCSM3). *Journal of Climate*, **19**, 2584–2596.

Körner C (2000) Biosphere responses to CO2 enrichment. *Ecological Applications*, **10**, 1590–1619.

Kroll JH, Ng NL, Murphy SM, Flagan RC, Seinfeld JH (2006) Secondary organic aerosol formation from isoprene photooxidation. *Environmental Science & Technology*, **40**, 1869–1877.

Lamb B, Gay D, Westberg H, Pierce T (1993) A biogenic hydrocarbon emission inventory for the USA using a simple forest canopy model. *Atmospheric Environment: Part A – General Topics*, **27**, 1673–1690.

Lathière J, Hauglustaine DA, De Noblet-Ducoudre N, Krinner G, Folberth GA (2005) Past and future changes in biogenic volatile organic compound emissions simulated with a global dynamic vegetation model. *Geophysical Research Letters*, **32**, doi: 10.1029/2005GL024164.

Lawrence PJ, Chase TN (2007) Representing a new MODIS consistent land surface in the Community Land Model (CLM 3.0). *Journal of Geophysical Research – Biogeosciences*, **112**, doi: 10.1029/2006JG000168.

Lelieveld J, Butler TM, Crowley JN *et al*. (2008) Atmospheric oxidation capacity sustained by a tropical forest. *Nature*, **452**, 737–740.

Liao H, Chen WT, Seinfeld JH (2006) Role of climate change in global predictions of future tropospheric ozone and aerosols. *Journal of Geophysical Research – Atmospheres*, **111**, doi: 10.1029/2005JD006852.

Loreto F, Mannozzi M, Maris C, Nascetti P, Ferranti F, Pasqualini S (2001) Ozone quenching properties of isoprene and its antioxidant role in leaves. *Plant Physiology*, **126**, 993–1000.

Meehl GA, Washington WM, Santer BD *et al*. (2006) Climate change projections for the twenty-first century and climate change commitment in the CCSM3. *Journal of Climate*, **19**, 2597–2616.

Mohan JE, Clark JS, Schlesinger WH (2007) Long-term CO2 enrichment of a forest ecosystem: implications for forest regeneration and succession. *Ecological Applications*, **17**, 1198–1212.

Monson RK, Fall R (1989) Isoprene emission from aspen leaves – influence of environment and relation to photosynthesis and photorespiration. *Plant Physiology*, **90**, 267–274.

Monson RK, Harley PC, Litvak ME, Wildermuth M, Guenther AB, Zimmerman PR, Fall R (1994) Environmental and developmental controls over the seasonal pattern of isoprene emission from aspen leaves. *Oecologia*, **99**, 260–270.

Monson RK, Jaeger CH, Adams WW, Driggers EM, Silver GM, Fall R (1992) Relationship among isoprene emission rate, photosynthesis, and isoprene synthase activity as influenced by temperature. *Plant Physiology*, **98**, 1175–1180.

Monson RK, Trahan N, Rosenstiel TN *et al*. (2007) Isoprene emission from terrestrial ecosystems in response to global change: minding the gap between models and observations. *Philosophical Transactions of the Royal Society A – Mathematical Physical and Engineering Sciences*, **365**, 1677–1695.

Niyogi D, Xue YK (2006) Soil moisture regulates the biological response of elevated atmospheric CO2 concentrations in a coupled atmosphere biosphere model. *Global and Planetary Change*, **54**, 94–108.

Oleson KW, Bonan G, Bosilovich M *et al*. (2004) Technical description of the Community Land Model (CLM). pp. 174. NCAR, Boulder, CO, USA.

Pegoraro E, Rey A, Greenberg J, Harley P, Grace J, Malhi Y, Guenther A (2004) Effect of drought on isoprene emission rates from leaves of Quercus virginiana Mill. *Atmospheric Environment*, **38**, 6149–6156.

Petit JR, Jouzel J, Raynaud D *et al*. (1999) Climate and atmospheric history of the past 420 000 years from the Vostok ice core, Antarctica. *Nature*, **399**, 429–436.

Petron G, Harley P, Greenberg J, Guenther A (2001) Seasonal temperature variations influence isoprene emission. *Geophysical Research Letters*, **28**, 1707–1710.

Possell M, Hewitt CN, Beerling DJ (2005) The effects of glacial atmospheric CO_2 concentrations and climate on isoprene emissions by vascular plants. *Global Change Biology*, **11**, 60–69.

Rasmussen RA, Went FW (1965) Volatile organic material of plant origin in the atmosphere. *Proceedings of the National Academy of Sciences of the United States of America*, **53**, 215–220.

Rosenstiel TN, Ebbets AL, Khatri WC, Fall R, Monson RK (2004) Induction of poplar leaf nitrate reductase: a test of extrachloroplastic control of isoprene emission rate. *Plant Biology*, **6**, 12–21.

Sanadze GA (1959) Excretion of organic volatile compounds by plants. *Bulletin of the Acadmy of Science, Georgia Soviet Socialist Republic*, **22**, 449–454.

Sanderson MG, Jones CD, Collins WJ, Johnson CE, Derwent RG (2003) Effect of climate change on isoprene emissions and surface ozone levels. *Geophysical Research Letters*, **30**, doi: 10.1029/2003GL017642.

Scholze M, Knorr W, Arnell NW, Prentice IC (2006) A climate-change risk analysis for world ecosystems. *Proceedings of the National Academy of Sciences of the United States of America*, **103**, 13116–13120.

Sharkey TD, Singsaas EL (1995) Why plants emit isoprene. *Nature*, **374**, 769–769.

Sharkey TD, Singsaas EL, Lerdau MT, Geron CD (1999) Weather effects on isoprene emission capacity and applications in emissions algorithms. *Ecological Applications*, **9**, 1132–1137.

Shindell DT, Faluvegi G, Bauer SE *et al.* (2007) Climate response to projected changes in short-lived species under an A1B scenario from 2000–2050 in the GISS climate model. *Journal of Geophysical Research – Atmospheres*, **112**, D20103, doi: 10.1029/2007JD008753.

Singsaas EL, Laporte MM, Shi JZ *et al.* (1999) Kinetics of leaf temperature fluctuation affect isoprene emission from red oak (Quercus rubra) leaves. *Tree Physiology*, **19**, 917–924.

Tao ZN, Jain AK (2005) Modeling of global biogenic emissions for key indirect greenhouse gases and their response to atmospheric CO2 increases and changes in land cover and climate. *Journal of Geophysical Research – Atmospheres*, **110**, doi: 10.1029/2005JD005874.

Thornton PE, Lamarque JF, Rosenbloom NA, Mahowald NM (2007) Influence of carbon–nitrogen cycle coupling on land model response to CO2 fertilization and climate variability. *Global Biogeochemical Cycles*, **21**, GB4018, doi: 10.1029/2006GB002868.

Thornton PE, Zimmermann NE (2007) An improved canopy integration scheme for a land surface model with prognostic canopy structure. *Journal of Climate*, **20**, 3902–3923.

Tingey DT, Evans R, Gumpertz M (1981) Effects of environmental conditions on isoprene emissions from live oak. *Planta*, **152**, 565–570.

Velikova V, Pinelli P, Pasqualini S, Reale L, Ferranti F, Loreto F (2005) Isoprene decreases the concentration of nitric oxide in leaves exposed to elevated ozone. *New Phytologist*, **166**, 419–426.

Wang KY, Shallcross DE (2000) Modelling terrestrial biogenic isoprene fluxes and their potential impact on global chemical species using a coupled LSM–CTM model. *Atmospheric Environment*, **34**, 2909–2925.

Wiedinmyer C, Guenther A, Harley P *et al.*), (eds) (2004) *Global Organic Emissions from Vegetation, in: Emissions of Atmospheric Trace Compounds*. Kluwer Publishing Co, Dordrecht, the Netherlands.

Wilkinson M, Monson RK, Trahan N *et al.* (2008) Leaf isoprene emission rate as a function of atmospheric CO2 concentration. *Global Change Biology*, submitted..